Enhanced Human–Machine Interface in Braking

Shinsuk Park and Thomas B. Sheridan, *Life Fellow, IEEE*

***Abstract*—Antilock brake system (ABS) technology with powerful electronic components has shown superior braking performance to conventional vehicles on test tracks. On real highways, however, the performance of the ABS-equipped car has been disappointing. The poor braking performance with ABS has resulted from the questionable design of the human–machine interface for the brake system. The goal of this study is to design brake systems that provide more intuitive brake control and proper braking-performance information for the driver. In this study automotive brake systems are modeled as a type of master–slave telemanipulator. Human force-displacement interaction at the brake pedal has a strong effect on braking performance. As a preliminary study in brake-system design, the characteristics of human leg motion and its underlying motor-control scheme are studied through experiments and simulations, and a model of braking motion by the driver's leg is developed. This paper proposes novel brake systems based on two new aspects. First, the mechanical impedance characteristics of the leg action of the driver are taken into consideration in designing the brake systems. Second, the brake systems provide the driver with kinesthetic feedback of braking conditions or performance. The effectiveness of the proposed designs in a combined driver–vehicle system is investigated using driving simulation.**

***Index Terms*—Brake system, braking motion, human motor control, teleoperator.**

I. Introduction

BRAKING performance of modern vehicles has been greatly improved, owing to the availability of powerful electronic components for antilock brake system (ABS) and stability-control systems. ABS provides the driver with an opportunity to steer out of emergencies by reducing the likelihood of wheel locking. The ABS, however, can save a life only if the driver knows how to use it. Unfortunately, many drivers do not understand how it should be operated. Indeed, the accident statistics report that the implementation of ABS does not necessarily improve or could even impair the safety of drivers [1], [2].

Why has the ABS, which is supposed to have superior performance to the conventional brake system, had a worse record? The response of drivers is mostly to blame. Studies indicate that, in panic-braking situations, some drivers do not really slam down on the brake pedal. To activate ABS in emergency stops the brake pedal should be pushed down (full-brake). However, it is reported that most drivers back off after their first stab, even if emergency braking is required. Some drivers with ABS-equipped cars tend to pump the pedals as if they were driving non-ABS vehicles, reducing ABS' effectiveness and even contributing to some accidents. Such human reactions when applying the brake pedal fail to take advantage of the major feature of ABS.

Then, what are the causes of this misuse? First, physical limitations of drivers seem to be one reason. It is reported that some people experience trouble in braking in an emergency; this is plausible for elderly people who are weaker in leg strength. Second, the vibration cues ABS delivers to the drivers are to partly blame. Traditionally, a vibration signal indicates a warning or malfunction rather normal functioning of machines. Some drivers are confused by the vibration cue associated with the normal activation of ABS. This suggests that braking performance with ABS can be improved by design of the human–machine interface.

The problems with ABS raise several questions. First, while braking appears to be a simple action, many drivers still have problems in managing the brake pedal. Little is known about the mechanisms of musculoskeletal motor control in the driver's braking motion; few studies have investigated this operation. Second, a brake system should be studied as a combined system including the driver in-the-loop, rather than in isolation. While, in principle, ABS alone has superior performance to non-ABS, the performance of ABS combined with the driver can be quite disappointing. The driver needs to be included in a closed-loop analysis.

In this paper, two novel brake systems are proposed after considering two aspects. First, characteristics of the human leg and its motion are measured, and the underlying motor control scheme is examined using numerical simulation of a mathematical model of the human leg. Based on the human leg motion analysis, the driver's initial braking motion is modeled as a preprogrammed action. Second, the two new brake designs employ the bilateral teleoperation concept (force feedback representing tire-road friction) rather than the unilateral control (force feedback of brake-cylinder pressure) employed in conventional brake systems. Teleoperator studies report that force feedback to the operator and the adaptive change of impedance at the master port enhance teleoperation performance [3], [4].

Recently, the automotive industry has adopted the concept of "drive-by-wire" inspired by fly-by-wire (FBW) flight control. In FBW aircraft, bulky mechanical linkages have been replaced by wires, and there is no direct energy flow between the pilot and the mechanical system. Owing to electric signaling between the control input device and the actuator, the "feel" of forces exerted on the aircraft control surfaces reflected back on the control stick must be artificially created. It has been proven that carefully tailored mechanical characteristics (or force-displacement relations) reflected to the control stick provide the pilot with subjective satisfaction as well as better maneuverability.

Manuscript received November 6, 2001; revised February 1, 2004 and February 12, 2004. This paper was recommended by Associate Editor W. A. Gruver.

S. Park is with the Department of Mechanical Engineering, Korea University, Seoul 136-701, Korea (e-mail: sspark@alum.mit.edu).

T. Sheridan is with the Department of Mechanical Engineering and the Department of Aeronautics and Astronautics, Massachusetts Institute of Technology, Cambridge, MA 02139 USA (e-mail: sheridan@mit.edu).

Digital Object Identifier 10.1109/TSMCA.2004.832813

1083-4427/04$20.00 © 2004 IEEE

Authorized licensed use limited to: MIT Libraries. Downloaded on August 12,2010 at 14:54:01 UTC from IEEE Xplore. Restrictions apply.

Studies in avionics may provide us with ideas on how we could improve the ease and safety of driving through automation and computerization. In FBW aircraft, the control stick delivers special force "feel" signal to the pilot when the plane is near stall. This kind of force feedback can also be applied to the design of brake systems.

In the proposed designs, brake-pedal stiffness is controlled depending on braking activation or the road-surface condition. Thus, adaptive change of the brake-pedal stiffness is intended to provide the driver with intuitive cues of braking activation or of road-surface condition—a softer pedal for a wet/icy road and a stiffer pedal for a dry road. In addition, the preprogrammed nature of emergency leg motions produces further depression of a soft brake pedal on a wet road, which is advantageous for ABS in an emergency situation on wet/icy roads. Braking performance of these proposed driver–vehicle systems is evaluated using a driving simulator. Road-condition awareness by the test drivers and situation adaptability by the driver–vehicle systems are used for braking-performance evaluation, and the performance of the new brake designs and conventional brake systems are compared.

II. Modeling of Human Braking Motion

A. Background on Human Movement Generation

A great number of studies have attempted to reveal the basic properties of the human neuromuscular control system, and yet were unable to explain the exact methods of translating the desired movement into the muscle activity required to generate it. It seems, however, natural to assume that certain fundamental principles underlie the organization and performance of human motor behavior. In human motor control, a multistaged process in transforming sensory input into motor output seems plausible and consistent with known neural architectures [5], [6]. It is argued that a multistage process is *hierarchically* organized with multiple levels ranging from an abstract specification of task goals to a concrete specification of motor neuron activities [7]. One of the common assumptions of hierarchical organization is that the production of motor behavior occurs in at least two stages: *planning* and *execution*. For many limb movements, motor planning appears to be represented and planned at a kinematic level. In his study in self-paced point-to-point movements by hand, Morasso [8] suggested that the central command for hand motion is formulated in body-centered Cartesian coordinates. Even if motor behavior is planned in terms of the kinematics of limb motion, the dynamics of the peripheral musculoskeletal system heavily influence the execution of that plan. Inertial dynamics introduces nonlinear coupling (the Coriolis and centrifugal forces) between body segments.

Then, how do humans circumvent the complexity of multilink dynamics? One possibility is the so-called "inverse dynamics" approach. Hollerbach and Atkeson [9] proposed that the central nervous system (CNS) solves the inverse kinematics problem to determine joint trajectories from the desired limb endpoint trajectory, then explicitly derives the necessary muscle forces using an inverse dynamics solution. It implies that the CNS explicitly performs an extremely demanding computation. An alternative approach assumes a look-up table instead of the complex computation [10], [11]. However, such tables may become very large, making this approach less likely. An alternative and simpler approach suggests that the CNS utilizes the effective dynamic and mechanical behavior of the muscles and neural feedback circuits to circumvent the computational complexities of coordinating multijoint motions. The muscles and neural control circuits have a "spring-like" property; the muscle force varies with muscle length under constant neural input. For a single joint, the combined action of a group of muscles spanning the joint, both agonists and antagonists, define an equilibrium posture for the joint. Central command may generate a series of equilibrium points for a limb, and the "spring-like" properties of the neuromuscular system will tend to drive the motion along a trajectory that follows these intermediate equilibrium postures. This *equilibrium point hypothesis* applies to the control of both static posture and voluntary movement [12].

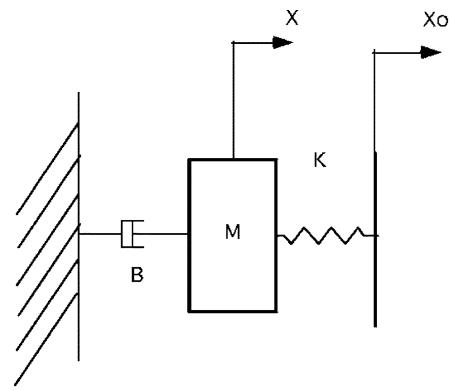

Fig. 1. One-dimensional model of equilibrium point control.

Fig. 1 illustrates a mechanism of the equilibrium point control in one-dimensional motion. In the figure mass M is driven by the force caused by stiffness K and damping B, and the difference between equilibrium position x_O and actual position x. Here, equilibrium position x_O serves as a control input to the simple mechanical system. Flash [13] demonstrated that the equilibrium point control can be used to model two-link planar reaching motions of the arm at moderate speeds. Using experimentally measured stiffness and the equilibrium point trajectories with a bell-shaped velocity profile, the simulations captured the kinematic features of experimentally measured trajectories.

In limb movements, the actual trajectory depends on environmental perturbations as well as the equilibrium-point trajectory, commanded impedance, and limb dynamics. Equilibrium-point control applies the same strategy to tasks requiring interaction with the environment, unrestrained motions, and the transition between the two. Control of contact force can also be achieved through the use of an equilibrium point. Simply moving the equilibrium point to a point within a contact object will cause the limb to exert a force on that object.

There have been years of controversy over the validity of the equilibrium-point control hypothesis. Many investigators argued against the equilibrium-point control hypothesis; they provided experimental evidence that the brain controls the movement, doing all the calculations to figure out all muscle activities [14], [15]. Indeed, there is considerable evidence that the motor-control system takes into account the dynamic

Authorized licensed use limited to: MIT Libraries. Downloaded on August 12,2010 at 14:54:01 UTC from IEEE Xplore. Restrictions apply.

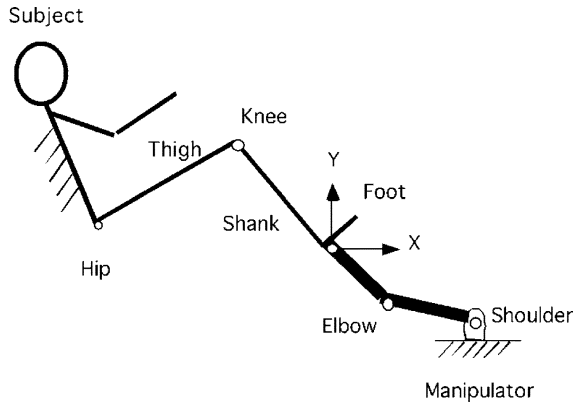

Fig. 2. Experimental setup for leg movement measurement.

properties of the limb as can be seen in preprogrammed or anticipatory reactions [16]. Other studies have attempted to eliminate the contrast between equilibrium hypothesis and inverse dynamics by suggesting the existence of motor primitives that generate force fields acting upon the limbs [17].

B. Human Leg Motion Analysis

As a precursor study for brake-system design, the characteristics of human leg motion and the underlying motor-control scheme were examined through experiments and simulations. In conventional brake pedals, the lever arm is pivoted from above the pedal, and this makes the driver's initial or emergency braking motion reduced to two degrees of freedom with free hip and knee joints and locked ankle joint [18]. In this study, a two degree-of-freedom *leg* motion was analyzed, as in a number of experimental and theoretical studies on planar *arm* motion [8], [13], [19], [20].

Characteristics of the human leg were explored through measurements of simple reaching motion, impulsive motion, and postural stiffness. Computer simulations of a mathematical model of the human leg were carried out to recreate the experimental result of a simple reaching motion.

1) Experiments on Human Leg: Fig. 2 shows a computer-controlled two-link manipulator and a human subject. The two-link manipulator measured the position of the foot and the force exerted by it. To eliminate the effect of gravity, subjects lay laterally so that their sagittal planes were parallel to the horizontal plane, and the movements of their legs were contained in the plane. The trunk of the subject was fixed to the table, serving as a base. The hip and knee joints were free to move allowing a two degree-of-freedom motion. A brace was used to lock the ankle joint at 90°.

The human subjects were all male affiliated with MIT, ranged in age from 21 to 31. The thigh and shank lengths of the subjects were measured, as well as their weights and heights. Based on the thigh and shank lengths along with foot position measured by the manipulator, hip and knee joint angles were calculated using inverse kinematics of two degree-of-freedom motion.

a) *Reaching Motion*: In this experiment, the subjects were instructed to move their feet between two *unspecified* targets as they would normally reach their feet from one point to another. Fig. 3 shows the trajectories of foot-reaching motion from four subjects. The trajectories were roughly straight. They show the same curvature, as if the center of curvature is placed in front of the subjects, while they all have different starting and finishing points. Fig. 4 shows velocities corresponding to the point-to-point movements. It is noteworthy that the velocity profiles have an asymmetric unimodal bell shape.

b) *Impulsive Motion*: In the impulsive movement experiment, subjects were instructed to make a series of sharp jerky motions or kick-and-return motions of the foot. It was reasoned that an impulse as an extremely abrupt movement would include the highest frequency components that the subject was capable of producing. Thus, power spectral density was used as an estimation of the bandwidth of foot motion. Rise times during impulsive motion were typically between 200 and 300 ms. The bandwidth of the motion was lower than 5 Hz. It was reported that rise time for a human arm motion is around 60 ms and that its bandwidth is between 20 and 30 Hz [21]. The results in this study showed much slower leg response. This probably results from the fact that the human leg has a larger inertia and longer limb length than the arm.

c) *Postural Stiffness*: The static components of the human leg impedance were measured by a procedure similar to the experiment used by Mussa–Ivaldi *et al.* [22] in their *arm* study. While no such tests had previously been performed for the *lower limb*, it seems reasonable to assume that common mechanisms apply to both the arm and the leg. The basic method is as follows: provide a perturbation that induces a displacement of the foot and then relate the evoked force to the input displacement to estimate the stiffness. After the foot of the subject was moved to a reference position, displacements were applied to the foot by a computer-controlled manipulator. The displacements were given in directions of 90°, 135°, and 180° from the x axis of the coordinate system defined in Fig. 2. The magnitude of these displacements ranged from 3 to 5 cm, and the resulting displacement and force imposed at the foot were recorded. During the procedure, the subject was instructed "not to resist voluntarily," so that only passive static response would be measured. From the data set collected in three directions, the stiffness field at the foot was estimated by the procedure similar to the experiment used by Mussa–Ivaldi *et al.* [22]. While the force-displacement function for muscle is fundamentally nonlinear, the function can be considered linear for small displacements about the equilibrium point. Therefore, the two-dimensional (2-D) relationship of the displacement and corresponding force can be expressed as

$$\begin{bmatrix} F_x \\ F_y \end{bmatrix} = -\begin{bmatrix} K_{xx} & K_{xy} \\ K_{yx} & K_{yy} \end{bmatrix} \begin{bmatrix} \Delta x \\ \Delta y \end{bmatrix} \tag{1}$$

where F_x and F_y are the components of the restoring force, Δx and are the components of the imposed displacement, and the elements of stiffness matrix, K_{xx}, K_{xy}, K_{yx}, and K_{yy}, are the linear stiffness terms in the posture. From three sets of force and displacement data measured in three directions, four elements of the linear stiffness matrix can be estimated.

Authorized licensed use limited to: MIT Libraries. Downloaded on August 12,2010 at 14:54:01 UTC from IEEE Xplore. Restrictions apply.

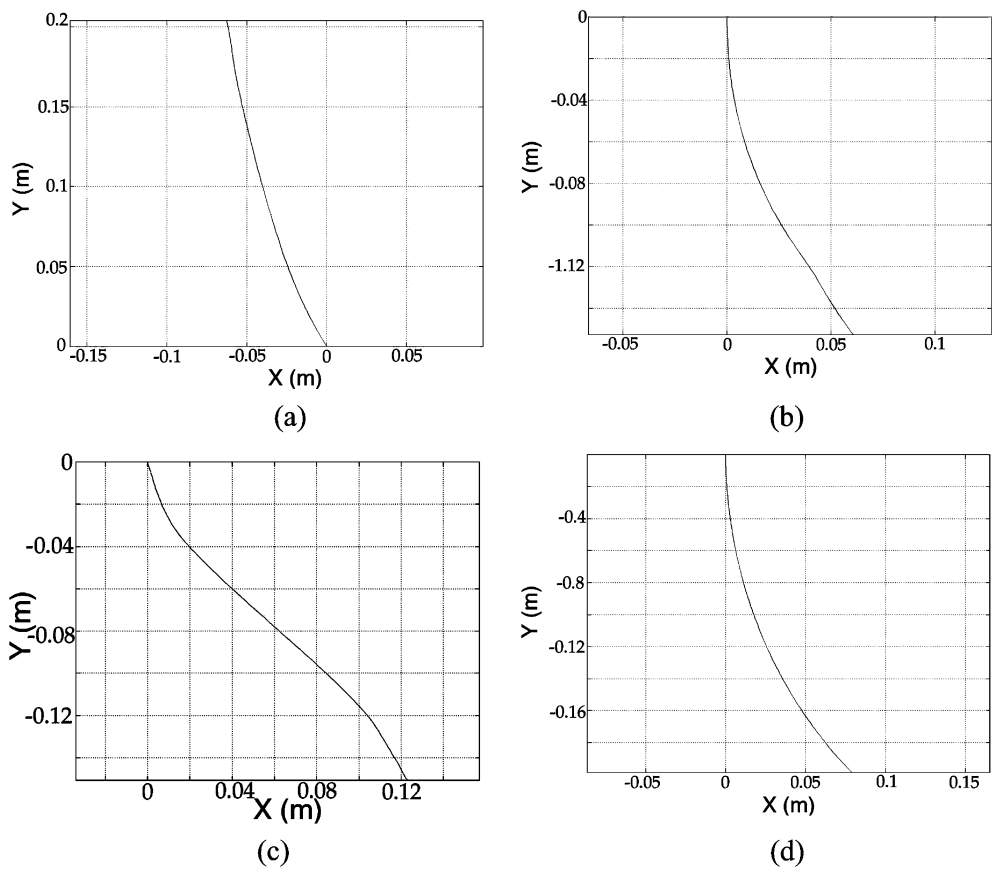

Fig. 3. Trajectories during foot-reaching motion. (a) Subject A. (b) Subject B. (c) Subject C. (d) Subject D. (Same coordinates as in Fig. 2).

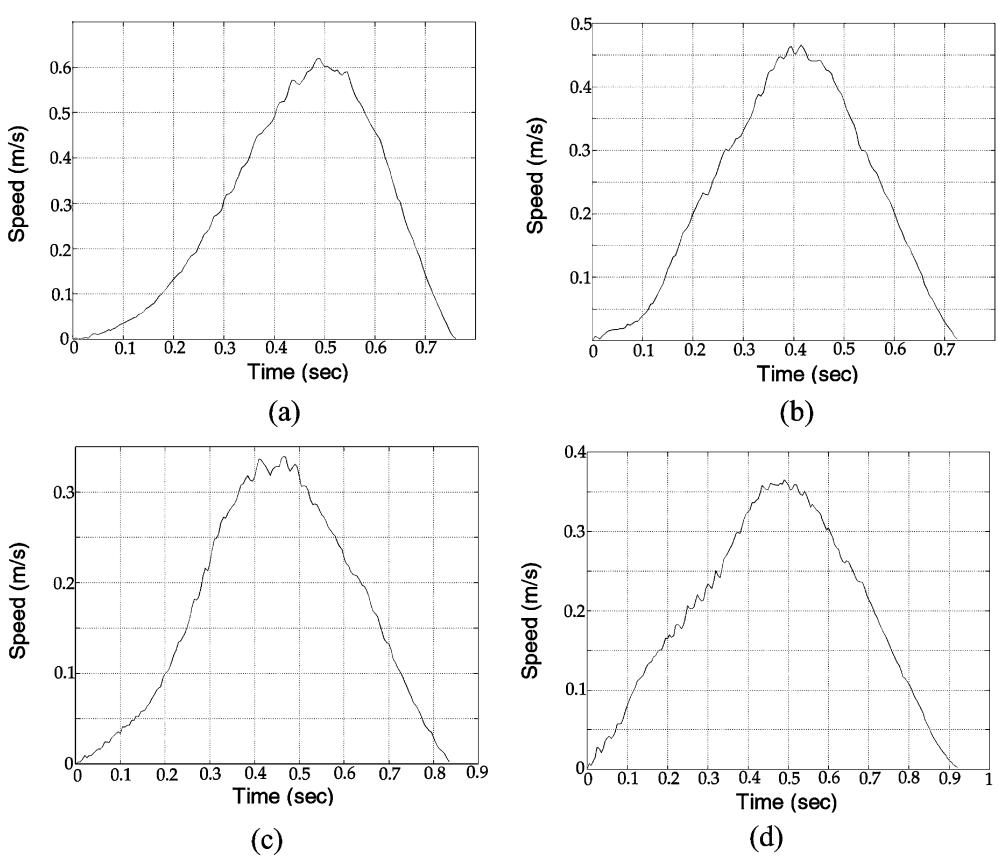

Fig. 4. Velocity profiles during foot-reaching motion. (a) Subject A. (b) Subject B. (c) Subject C. (d) Subject D.

Authorized licensed use limited to: MIT Libraries. Downloaded on August 12,2010 at 14:54:01 UTC from IEEE Xplore. Restrictions apply.

TABLE I
JOINT-STIFFNESS MATRICES

Subject	Joint stiffness matrix (Nm/rad)	Eigensolution Eigenvalue (Direction of Eigenvector)
A	$\begin{bmatrix} 642.1 & -511.1 \\ -478.0 & 387.8 \end{bmatrix}$	Major: 1025.4 (-36.9°) Minor: 4.6 (51.3°)
B	$\begin{bmatrix} 616.8 & -366.3 \\ -468.8 & 279.3 \end{bmatrix}$	Major: 895.5 (-37.3°) Minor: 0.6 (59.3°)
C	$\begin{bmatrix} 778.0 & -574.7 \\ -565.8 & 459.1 \end{bmatrix}$	Major: 1208.1 (-37.1°) Minor: 25.0 (52.5°)
D	$\begin{bmatrix} 849.3 & -583.6 \\ -609.0 & 418.5 \end{bmatrix}$	Major: 1267.8 (-35.6°) Minor: 0.0052 (55.5°)

The endpoint stiffness field measured at a reference posture can be transformed into the stiffness in joint space using the leg Jacobian matrix J_L, which is calculated using the measured foot position and inverse kinematics of two degree-of-freedom leg model. The joint stiffness K_J can be estimated as follows:

$$K_J = J_L^T K J_L. \tag{2}$$

The estimated joint matrices are given in Table I. The joint matrices appear to be nearly symmetric. The directions represent the angle between the major and horizontal axes in joint space. The directions of the major axes point approximately –35° for all the subjects. When the endpoint stiffness is transformed into the joint stiffness, the minor stiffness becomes even smaller compared to the major stiffness. Note that the stiffness of four subjects have similar major and minor eigenvalues.

The symmetric component of the stiffness matrix $\left(K_{J,symm} = (K_J + K_J^T/2)\right)$ can be graphically represented as an ellipse characterized by the magnitude (area of ellipse), shape (the ratio of major and minor axes), and the orientation (direction of the major axis). In their arm stiffness study, Mussa–Ivaldi *et al.* [22] postulated that the shape and orientation of the stiffness ellipse in joint space is invariant over all subjects tested. This consistency in joint space can also be found in the leg stiffness.

2) Simulation of Mathematical Model: The findings from the experiments raise a question of whether there exists a simple motor program in human leg movement. One of the possible candidates is the equilibrium-point hypothesis [23], [24]. Computer simulations of a mathematical model were performed to recreate the experimental results of reaching motion of the human leg in the framework of the equilibrium point control hypothesis.

a) Mathematical Modeling: The two-link planar model of the lower limb, shown in Fig. 5, is constrained to move in the sagittal plane, and has two degrees of freedom corresponding to the knee and hip joints. Based on the data of the subject's height, weight and limb lengths, the distribution of the mass and inertial moment among the body segments was estimated using a regression model [25]. The thigh and shank-foot segments have masses m_1 and m_2, respectively. Likewise, the respective centroidal moments of inertia are I_1 and I_2. The angular convention Φ defines the relative joint flexion between adjacent segments.

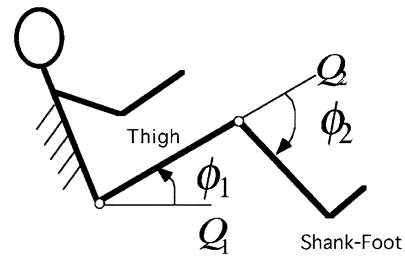

Fig. 5. Two-link model of human leg.

The joint torques corresponding to these joint angles are denoted by Q. Therefore, flexional torques are positive, adhering to the angular convention. The general form for the dynamics equations is given as follows:

$$H(\Phi)\ddot{\Phi} + h(\Phi, \dot{\Phi}) + G(\Phi) = Q = Q_{\text{act}} + Q_{\text{ext}} \tag{3}$$

where

$H(\Phi)$	2×2 moment of inertia matrix;
$h(\Phi, \dot{\Phi})$	2×1 rate-dependent vector;
$G(\Phi)$	2×1 gravitational vector;
Q_{act}	2×1 torque vector by muscles forces;
Q_{ext}	2×1 torque vector by external forces.

Here, the configuration of the dependent inertia matrix $H(\Phi)$ and rate dependent gyroscopic terms $h(\Phi, \dot{\Phi})$ are functions of the segment masses, locations of segment mass centers, joint angles, and joint velocity. The gravitational terms $G(\Phi)$ are zero since the sagittal plane is in the horizontal plane.

While muscle force is a complicated function with many variables, the mechanical property of a muscle may be simplified to be a function of muscle length and its rate of change. Hence, leg muscle groups may be modeled as a combination of linear torsional springs and dampers as postulated in the arm models by Flash [13] and Won and Hogan [20]. Thus, the resultant actuation torques are assumed to be dependent only on deviation of the actual trajectory from the equilibrium point trajectory and on joint velocity. The following equation gives the joint control torques as a function of the instantaneous difference of actual and equilibrium point trajectories and joint velocity

$$\begin{aligned} Q_{\text{act}} &= -K_J(\Phi - \Phi_O) - B_J\dot{\Phi} \\ K_J &= \begin{bmatrix} k_{HH} & k_{HK} \\ k_{KH} & k_{KK} \end{bmatrix} \\ B_J &= \begin{bmatrix} b_{HH} & b_{HK} \\ b_{KH} & b_{KK} \end{bmatrix} \end{aligned} \tag{4}$$

where

Q_{act}	torque vector of muscle forces;
Φ, $\dot{\Phi}$	vector of joint angles and rates;
Φ_O	vector of equilibrium-point joint angles;
K_J	joint-stiffness matrix;
B_J	joint-damping matrix.

Here, subscripts H and K denote hip and knee joints, respectively.

Additional assumptions for the equilibrium point control (EPC) model in foot-reaching motion are as follows. Stiffness matrix K_J and damping matrix B_J are assumed to be linear about the equilibrium position and the velocity, respectively.

Authorized licensed use limited to: MIT Libraries. Downloaded on August 12,2010 at 14:54:01 UTC from IEEE Xplore. Restrictions apply.

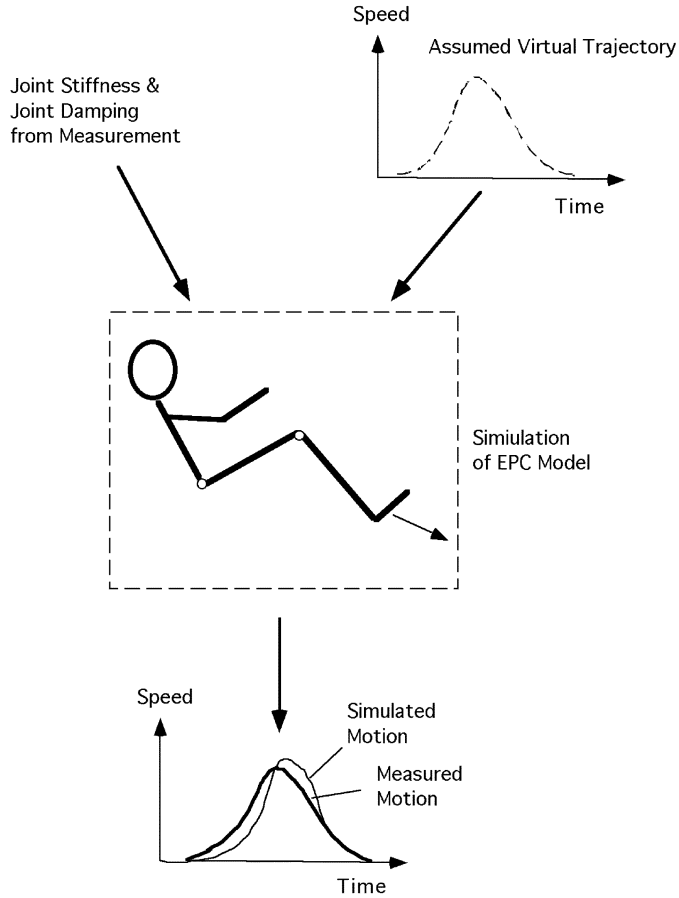

Fig. 6. Simulation procedure for foot-reaching motion.

They are also constant over the entire range of movements regardless of the posture. The driving input to the EPC model is an equilibrium-point trajectory that is a straight line in Cartesian space from the initial position x_i to the final position x_f. This trajectory has a minimum-jerk velocity profile taking the equilibrium point from the start to the finish

$$x(t) = x_i + (x_f - x_i)(10\tau^3 - 15\tau^4 + 6\tau^5) \tag{5}$$

$$v(t) = (x_f - x_i)\frac{(30\tau^2 - 60\tau^3 + 30\tau^4)}{t_f}. \tag{6}$$

Here, τ is normalized time ($\tau = t/t_f$), and t_f is the duration of movement. Motor programs for all reaching movements of the EPC model can be generated simply by translating and scaling the minimum-jerk functions described above.

b) Simulation of Foot-Reaching Movement: With a minimum-jerk equilibrium point trajectory and the measured postural stiffness as simulation inputs, a point-to-point reaching motion under no external forces was recreated and compared with the experimentally measured movement. This procedure is similar to works of Flash [13] for arm movement. Fig. 6 illustrates the simulation procedure. The equilibrium point trajectory in Cartesian coordinates is transformed into leg joint coordinates Φ using the geometry of the two-link leg model. Under the assumption that stiffness is greater in motion than in static posture, the value of each element in the measured stiffness matrix was multiplied by a scaling factor. The scaling factor ranged between 9 and 13 for outward reaching motion. For inward motion, the scaling factor was around five. Also, the damping matrix is assumed to be proportional to the scaled stiffness matrix with a time constant $\tau = B_J/K_J$. The time constant was chosen to be 0.05 s as in works of Flash [13] and Won and Hogan [20] for arm movement.

Simulation results from four subjects are shown in Figs. 7 and 8. Fig. 7 compares the simulated trajectories with the actual trajectories from measurement. All the motions were outward, with the exception of subject A. While the simulated paths closely resemble the measured ones, the paths resulting from the simulations failed to reproduce the unique curvature existent in those from measurement. Fig. 8 compares simulated and measured velocity profiles. While the simulations produced the typical bell-shaped velocity profiles, the profile peaks did not coincide with those of measured velocities.

Simulated trajectories showed kinematic features such as straight paths and bell-shaped velocity profiles. With a single minimum-jerk equilibrium trajectory as an input, the features of simulated trajectories paralleled those of measured movement.

C. Modeling of Braking Motion

Sections II-A and B examined the general features of human leg motion through experiments and numerical simulation. The point-to-point movement by the foot showed nearly identical features to those of planar *hand* reaching motion demonstrated in previous arm experiments [8], [13], [19]. While all the trajectories of foot-reaching movements were fairly straight, movements with a locked ankle showed unique curvature. The velocity profile during point-to-point motion had a characteristic bell shape. Arm-movement experiments showed that the hand of the subject generates essentially a straight path from start to finish, with a characteristic bell-shaped tangential velocity profile during self-placed point-to-point reaching movements [8], [19]. The features found in experiments were similar to those that can be found in arm-motion studies [13], [22]. In her arm-movement simulations, Flash [13] showed that the equilibrium-point control hypothesis is competent to predict simple point-to-point reaching motion. As one of the candidates for the motor program producing foot-reaching motion, this equilibrium-point control hypothesis was tested by numerical simulations. The equilibrium point control model seems to consistently recreate experimental results.

As postulated by Flash [13] in her arm motion study, simple foot-reaching motions may be controlled by a single equilibrium point trajectory. Won and Hogan [20] also suggested that a *single* control scheme generates movements with or without external perturbations, by showing that there exists a moving attractor point that automatically restores the arm motion to the unperturbed path under unexpected perturbations.

In conventional brake pedals, the lever arm pivoted from above the pedal makes the action path of the pedal close to the natural path of the foot. It allows the driver to produce his maximum leverage [18]. The leg motion with a locked ankle showed the same curvature as that of the pedal action path.

Simulation of the EPC model in Section II-B suggests the open-loop nature in foot-reaching motion. From the general leg-

Authorized licensed use limited to: MIT Libraries. Downloaded on August 12,2010 at 14:54:01 UTC from IEEE Xplore. Restrictions apply.

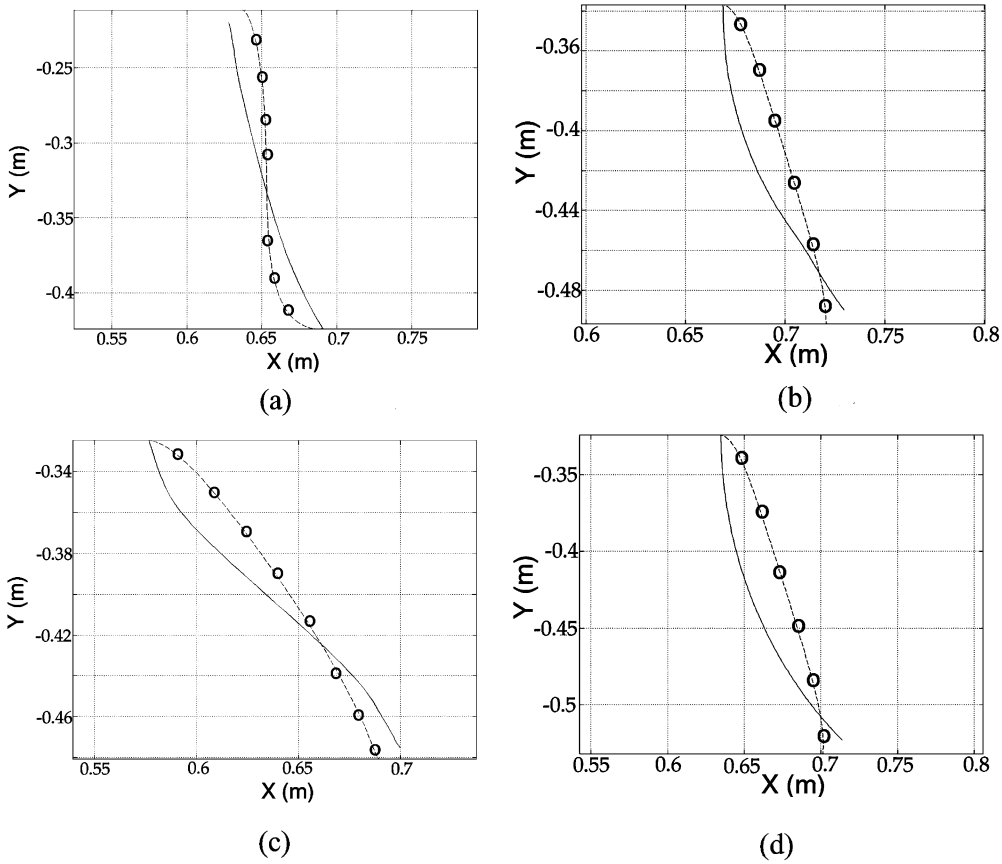

Fig. 7. Comparison of trajectories from measurement and simulation. (a) Subject A. (b) Subject B. (c) Subject C. (d) Subject D. (solid line: measured trajectory, dotted line: simulated trajectory).

motion analysis and features of the brake pedal, the emergency braking motion by a human leg can be modeled as follows.

- Braking motion has two degrees of freedom with free hip and knee joints.
- Initial braking motion is a simple open-loop reaching motion by the foot with no visual target.
- Braking motion is a movement in free space was followed by contact with the brake pedal.
- Braking motion is a preprogrammed motion with no closed-loop feedback until after initial brake-pedal depression.

The fact of preprogrammed braking motion suggests that drivers have the same command from the CNS in movements both in free space and in contact with the brake pedal. It also implies the same motor commands for different brake-pedal impedances. Further pedal depression will be induced with a softer brake pedal with the same CNS command. This assumption is key to proposed brake-system designs in Section III.

III. Design of Brake System as Teleoperator

A. Background on Teleoperators

Sheridan [26] defined a *teleoperator* as "a machine that extends a person's sensing and/or manipulating capability to a location remote from that person." A master–slave manipulator is a teleoperator, where the manipulator mimics the operator's own motions, usually hand motions. The human operator, the master–slave manipulator, and the remote task comprise a remote manipulation system. At the master port, the master–slave manipulator interacts with the operator; at the slave port it interacts with the task in the remote environment. The important variables in the interactions are those that describe the power flow: the contact forces and the velocities (and positions). Raju [3] suggested that the master–slave manipulator be modeled as a two-port mechanical system, analogous to two-port electrical networks. Fig. 9 shows the electrical network model of the remote manipulation system: the human operator, the master–slave manipulator, and the task [3].

One of the technical issues in teleoperation is how to reproduce the bidirectional properties of mechanical energy flow. The term "force feedback" suggests that the teleoperator senses velocity or position of the operator's limb and applies the appropriate force to the human operator. The operator's positioning tool (joystick or handgrip) can be driven to apply reaction forces to the operator's hand while he attempts to move it to the desired position, so that the operator feels as though he is applying the force to the environment directly.

The level of force feedback that the operator feels can be determined by the specification of the master port impedance, where a generalized mechanical impedance is defined as the relation between applied force and velocity along with its time-derivatives and time integrals. Raju [3] showed that it is advantageous to adjust master and slave impedances depending on the task characteristics. In a contact task using the teleoperator, before the manipulator makes contact with the task object, the

Authorized licensed use limited to: MIT Libraries. Downloaded on August 12,2010 at 14:54:01 UTC from IEEE Xplore. Restrictions apply.

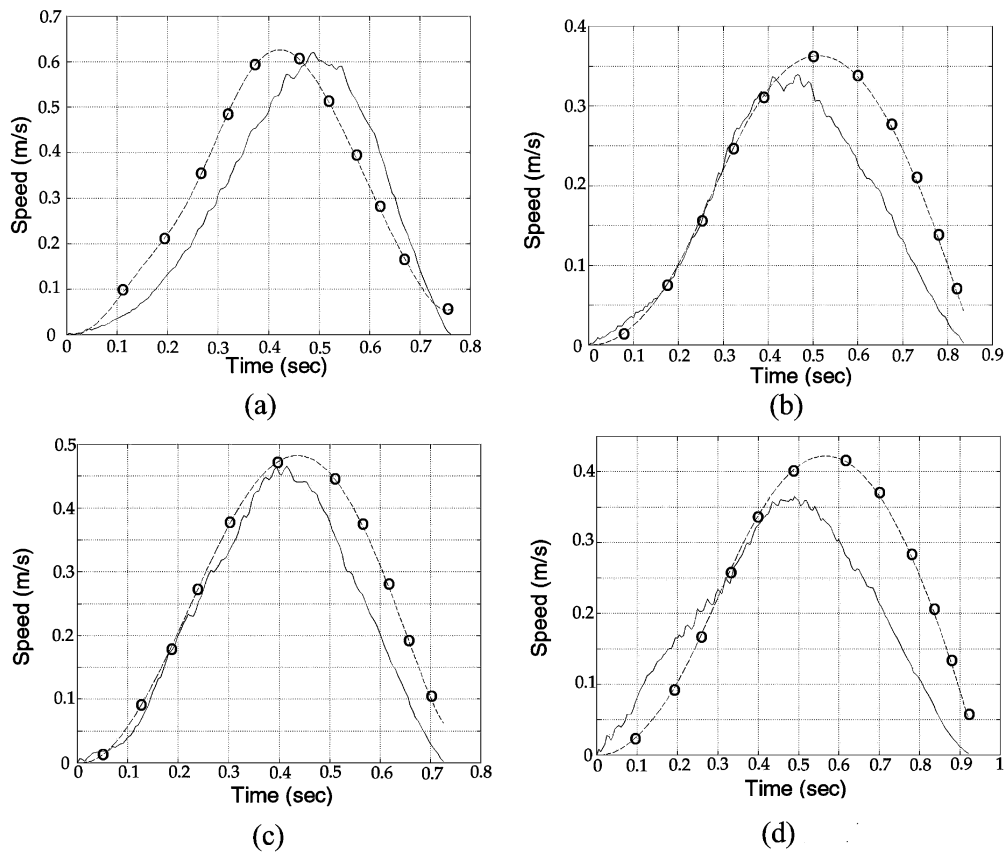

Fig. 8. Comparison of velocity profiles from measurement and simulation. (a) Subject A. (b) Subject B. (c) Subject C. (d) Subject D. (solid line: measured trajectory, dotted line: simulated trajectory).

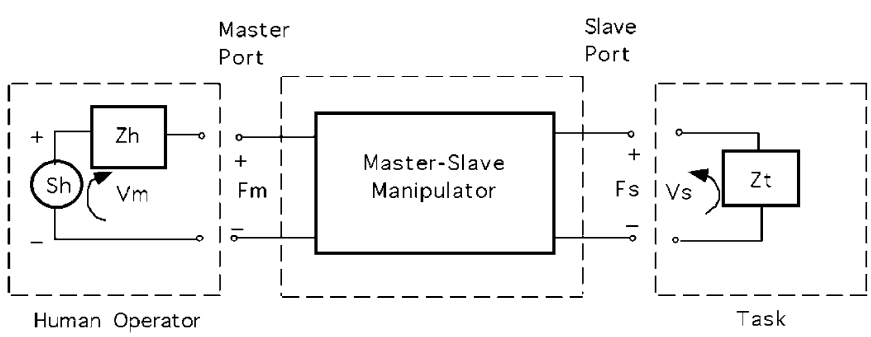

Fig. 9. Network model of a remote manipulator system [3].

slave-port impedance should be low, while the master port impedance should be high, so that contact can be sensed but without the excessive force on the task object. After contact, the slave-port impedance should be increased so that the task can be executed with adequate position control, while the master port impedance should be reduced to provide a comfortable yet adequate level of force feedback to the operator. The selection of impedance at master and slave ports, depending on the characteristics of the operator and the task, is an area to be explored further.

B. Modeling of Brake System as a Teleoperator

While manual or hand controls are more widely employed than foot controls in operating machines, a pedal is used in conventional vehicle brake systems. To produce a desired pedal displacement, the driver must produce a force determined by the mechanical stiffness or impedance of the brake pedal; to produce a desired force requires a particular displacement, also determined by the impedance. The impedance characteristic of the brake pedal may have a strong effect on the driver's braking performance.

While control of conventional brake systems is performed initially in an open-loop manner, the brake system can be modeled as a teleoperator with poor performance feedback to the operator, where at the tire-road interface the braking task is performed by the driver at a *remote* location using the brake pedal. The foot-pedal interface can be modeled as a master port, and tire-road interface as a slave port.

In understanding brake activation, knowledge of the tire-road interface is essential. The braking force generated at a wheel of

Authorized licensed use limited to: MIT Libraries. Downloaded on August 12,2010 at 14:54:01 UTC from IEEE Xplore. Restrictions apply.

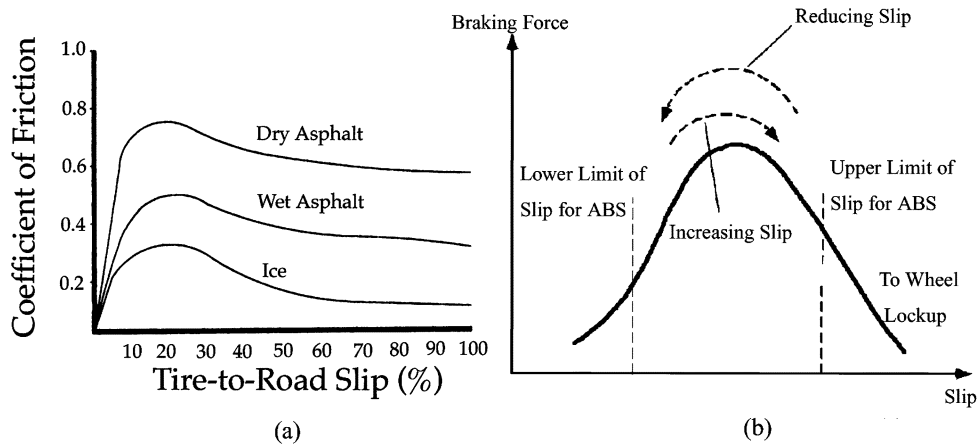

Fig. 10. Relationship of road condition, wheel slip, and braking force. (a) Friction coefficient-slip ratio curves on various road-surface conditions. (b) Braking force-slip relationship of brake system during ABS activation.

a vehicle is the product of the normal force on the wheel and the coefficient of friction between the tire and the road. The friction coefficient of the tire-road contact is not a constant, but rather a function of the road-surface condition and the relative slip between the tire and the road. Wheel slip is the difference between rolling speed and forward speed of the wheel. Fig. 10(a) illustrates curves relating the friction coefficient to wheel slip on various road surfaces. As can be seen in the figure, the magnitude of the peak in the friction coefficient curves varies widely with road conditions. The friction coefficient has its maximum value when the slip ratio is around 0.2. Note that beyond the peak friction coefficient on a given road condition, the slope of the curve becomes negative. Beyond this point, more pedal force without proper slip control results in less braking. The main function of an ABS is to keep the friction coefficient at or near its maximum, which will in turn lead to shorter stopping distance and better maneuverability. In ABS, when a sensor at a wheel detects the impeding lockup of the wheel, the brake pressure is modulated to keep the friction coefficient or frictional braking force near its maximum value. Fig. 10(b) illustrates braking force versus wheel slip during ABS activation. As the brake pressure is applied, braking torque applied by the brake system increases and the angular speed of the wheel decreases, causing the wheel slip to increase. The braking force at tire-road interface increases to reach its peak value as the wheel slip increases. After the peak braking force is reached, the control unit commands the modulator to reduce the brake pressure. As the brake pressure is reduced, wheel slip is reduced and the braking force again passes through the peak.

If ABS is modeled as a teleoperator (Fig. 11), the braking task in an automobile is analogous to a contact task or to grabbing an object using a telemanipulator. In grabbing an object using such a teleoperator, the operator should apply enough force on the handgrip or joystick to achieve enough contact force between the telemanipulator and the task object. In a braking task using ABS, the driver should apply enough force to the brake pedal to achieve enough braking force at tire-road contact. Keeping the maximum braking force in ABS can be considered as keeping enough contact force with the task object in teleoperation. Upon activation of ABS, the tire-road contact gets a firmer grip. In

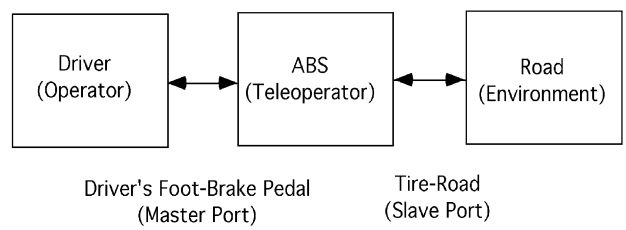

Fig. 11. Brake system as a teleoperator.

ABS, the signal indicating maximum braking is a nonintuitive vibration from the brake pedal; in teleoperation contact with a task object can be sensed by force feedback to the operator. As noted earlier it is believed that the required force with force feedback can be achieved by change of impedance at the master port or the brake pedal.

Though a visual or auditory signal could also be provided, force feedback or kinesthetic display appears to be more promising in the braking task, since the driver's visual or auditory sense is usually occupied by other information. While most importance is typically placed on our visual sense of the environment, it is the kinesthetic sense that provides us with much of the information necessary to modify and manipulate the world around us. There is a fundamental difference between kinesthetic information and that of visual and auditory displays. The visual and auditory channels are unidirectional information flows, and they do not involve energetic interaction in the physical variables being sensed [27]. In the kinesthetic channel, a transfer of energy is involved, and this enables the joystick or brake pedal to serve as a *kinesthetic display* as well as an *input device*.

C. New Brake-System Designs

Based on teleoperator principles, two new brake systems are proposed here. For design of new brake systems, two aspects are considered: 1) the driver's braking motion as described in Section II and 2) force feedback in teleoperation as discussed in the Section III-B.

1) Proposed Design 1: This system employs the same ABS components as currently, except that it has a servo system to

Authorized licensed use limited to: MIT Libraries. Downloaded on August 12,2010 at 14:54:01 UTC from IEEE Xplore. Restrictions apply.

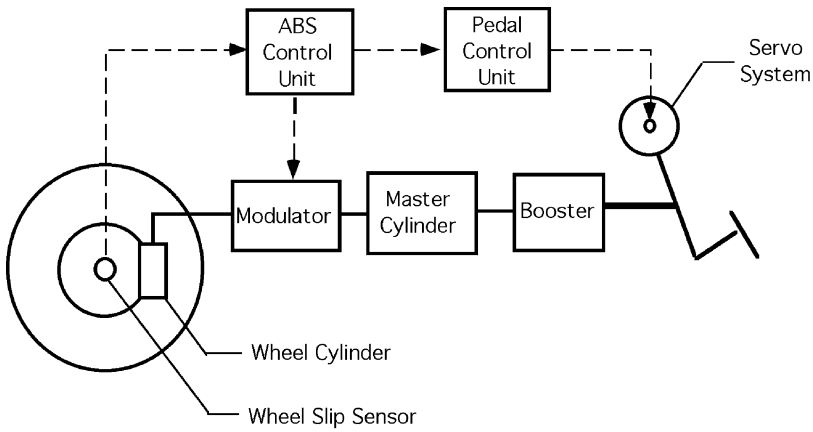

Fig. 12. Schematic view of design 1.

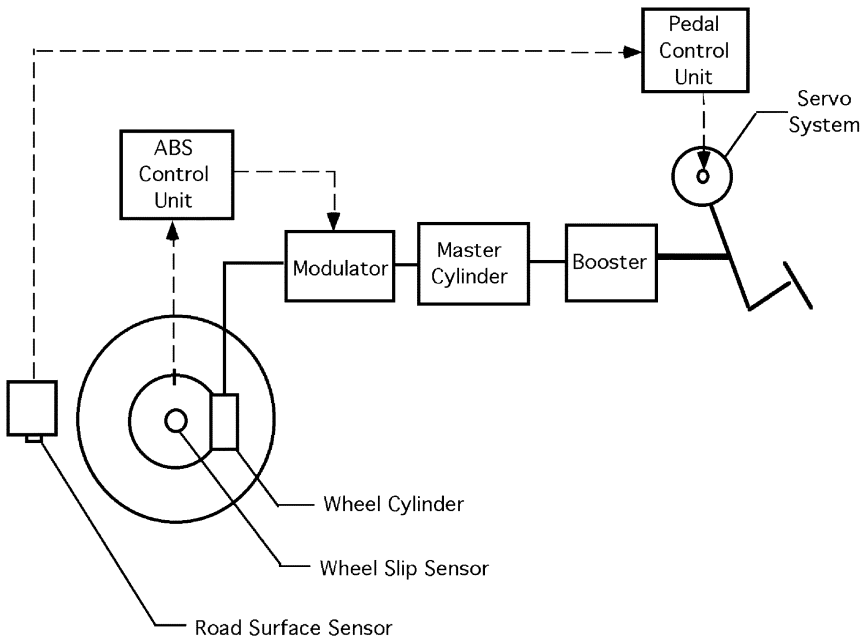

Fig. 13. Schematic view of design 2.

change the pedal impedance while filtering out the pulsing of the pedal on ABS activation. Upon detection of wheel slippage by ABS sensors, the brake pedal is tuned to be softer. On a wet/icy road, the driver can sense yielding of the pedal instead of vibration from it. If the braking motion of the driver is preprogrammed, a sudden change of the brake-pedal impedance will induce further depression of the pedal, which is advantageous in ABS since full pedal depression induces ABS activation on a wet/icy road. This design is analogous to the teleoperator with adaptive impedance at the master port performing a contact task. For the teleoperator contact task, Raju [3] suggested softer master impedance and stiffer slave impedance upon contact. This idea is directly applied to brake-system design; upon activation of ABS, brake-pedal impedance is tuned softer while tire-road contact gets firmer. Fig. 12 illustrates this brake-system design.

2) Proposed Design 2: Current development of optoelectronic sensors allows us to detect the road-surface condition as well as wheel slippage as in ABS. This sensor uses backscattered and reflected light information to detect the presence of ice, water, or mud on the road surface [28]. This proposed brake system employs the road-surface sensor to control the brake-pedal impedance in addition to the usual components of ABS, including the wheel-slip sensor. In the proposed design, upon detection of a wet/icy road, the impedance of the brake pedal is tuned softer. The driver is able to sense the road condition as he presses down on the pedal. This system is similar to a power steering wheel on an icy road; the steering wheel can be turned more easily on an icy road than on a dry road. This system depends on the correct sensing of the road-surface condition. Fig. 13 illustrates this brake-system design.

D. Simulator Tests

To test the applicability of the proposed brake designs, a simple driving simulator was developed for braking simulation. Using this braking simulator, the performance of new designs was evaluated and compared with that of conventional brake systems.

Authorized licensed use limited to: MIT Libraries. Downloaded on August 12,2010 at 14:54:01 UTC from IEEE Xplore. Restrictions apply.

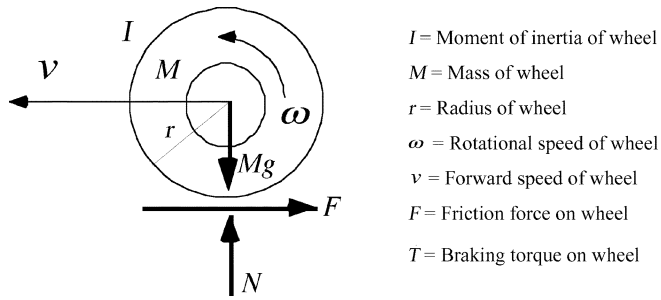

Fig. 14. Two degree-of-freedom vehicle model.

1) Simulator Setup: The simulator developed for this study was a simplified version of a fixed-base driving simulator. The whole simulation system was under control of a Pentium-based PC computer, which managed the hardware control, visual display, and braking-situation sequence encountered by the driver.

The PC processed the brake-pedal position or command signal by calculating vehicle and brake-system dynamics to yield vehicle motion on a visual display, namely the relative size of an object representing a leading car. While an active gas pedal was not provided in the simulator (only a foot rest from where the test driver moved his foot to brake), the speed of the car was gradually accelerated back to the reference speed upon release of the brake pedal. A speedometer was also provided to indicate the speed of the driver car. All this information was displayed on the PC monitor screen in front of the driver. The screen was updated at about 20 frames/s yielding the minimum smooth motion. To produce a relatively large brake-pedal force, an AC motor was used, and the motor output torque was also controlled by the PC. Braking conditions were fed back to the driver mainly by the visual display of the leading car. An additional cue to braking conditions was provided by controlling the pedal force exerted on the driver's foot.

2) System Modeling: The braking simulator used a simple two degree-of-freedom model for vehicle motion [29]. Fig. 14 shows the variables in the model developed for this simulator. Friction force on the wheel was modeled as a function of road-surface condition and wheel slip

$$F = \mu(\lambda) Mg \tag{7}$$

$$\lambda = \frac{v - r\omega}{v} \tag{8}$$

where μ and λ denote friction coefficient of road and wheel slip ratio, respectively.

The brake-system model employed by the braking simulator consisted of a vacuum booster, a master cylinder, a wheel cylinder, and a brake pad. The relationship between pedal displacement and booster output force was modeled as a first-order system as follows:

$$\frac{F}{X} = \frac{K_1}{\tau_1 s + 1}. \tag{9}$$

Here, F and X denote vacuum-booster output force and brake-pedal displacement, respectively.

Brake-system hydraulics between master cylinder and wheel cylinder were also modeled as a first-order system [29]:

$$\frac{P}{P^*} = \frac{K_2}{\tau_2 s + 1} \tag{10}$$

where P, P^* denote brake pressure at wheel cylinder and pressure at master cylinder, respectively.

The relationship between wheel cylinder pressure and brake torque was approximated to be linear

$$T = Kp \tag{11}$$

where K is brake gain or brake effectiveness.

For ABS, brake pressure was modulated depending on the wheel slip. This braking simulator used a simple logic of ABS activation: when wheel slip exceeded a threshold, brake pressure was relieved. The ABS cycle in the driving simulator was around 10 Hz, which is similar to that of a conventional ABS.

3) Test Models: Vehicle models with five different brake systems were tested using the brake simulator. The brake systems consisted of three conventional brake systems and the two new brake systems described in Section III-C. The test models used were as follows.

Model 1: This model was a passenger car that was not equipped with ABS.

Model 2: This model was a passenger car equipped with a conventional ABS. Activation of the ABS was cued by vibration at the brake pedal.

Model 3: This model was a passenger car equipped with an ABS and servo system to control brake-pedal stiffness. Stiffness of the brake pedal was softened 50% upon activation of the ABS instead of the vibration as in Model 2.

Model 4: This model was a passenger car equipped with ABS and a road-surface condition sensor. Upon detection of a wet/icy road surface, the stiffness of the brake pedal was reduced by 50%. This model assumed detection of road-surface condition by a perfect sensor.

Model 5: The last model was a passenger car equipped with an ABS. While the ABS functioned normally, the vibration at the brake pedal was filtered out in this model.

4) Experimental Tasks: The performances of the five brake systems described above were tested using the driving simulator. Road-condition awareness and situation adaptability of the drivers were evaluated under different braking situations and road-surface conditions.

In the simulator, the driver followed one lead car at a speed of 100 km/h trying to keep a 2-s headway before the lead car and, at a random time, braked to stop. The driver was able to control the speed of the driving car only through the brake pedal. In the first experiment, the *emergency-braking experiment*, the driver was instructed to follow the lead car on a dry or a wet/icy road and, upon a signal (representing lead car brake lights), to brake as quickly as possible. For the second experiment, the *pedal-pumping experiment*, the driver was instructed to follow the lead car on a dry or a wet/icy road and on the signal to pump the brake pedal to stop the car. In the

Authorized licensed use limited to: MIT Libraries. Downloaded on August 12,2010 at 14:54:01 UTC from IEEE Xplore. Restrictions apply.

TABLE II
RATING SYSTEM FOR SITUATION-ADAPTATION EXPERIMENT

Situation	Rating (0 to 2)
Gentle braking	If Distance to lead car when stopped < Initial headway: 2×(1 – Distance to lead car when stopped/Initial headway)
	If Distance to lead car when stopped > Initial headway: 0
Emergency braking	If no collision occurred: 2
	If Speed at collision < 48 km/h: 2×(1-Speed at collision/48 km/h)
	If Speed at collision > 48 km/h: 0

last experiment, the *situation-adaptation experiment*, the simulation produced various braking situations according to erratic behavior of the lead car and road conditions. In this case, drivers were instructed to follow the lead car and to react as they would in an actual driving situation. In this experiment, four situations were devised combining two different lead car behaviors and two different road-surface conditions: 1) gentle braking on a dry road, gentle braking on a wet/icy road, emergency braking on a dry road and 2) emergency braking on a wet/icy road. During a test run, the four situations appeared in random order.

In all experiments, the driver was asked to estimate the road-surface condition and decide whether it was dry or wet/icy. The driver's estimates were rated on a five point scale. The driver could choose one of five different responses: definitely dry, maybe dry, undeterminable, maybe wet/icy, and definitely wet/icy. When the estimate was correct with certainty, it was scored $+2$. When the estimate was correct but without certainty, the score was $+1$. When the driver was not able to recognize the road-surface condition at all, the score was 0. If the driver was uncertain about the estimate, and the estimate was incorrect, it was scored -1. If the driver was certain about the estimate, while it was incorrect, the score was -2. For example, if the driver chose "maybe dry" as his response, while the actual road condition was wet, the score for his estimation was -1.

In the *situation-adaptation experiment*, the adaptability to four situations that randomly appeared was rated. In the emergency-braking situation, the driver's task was to avoid rear-end collisions. In the gentle-braking situation, the driver's task was to stop the car as close to the lead car as possible without collision. Either collision with the lead car or excessive braking in the gentle-braking situation was considered to be a failure in situation adaptation. Table II illustrates the rating system for the *situation-adaptation experiment*.

The drivers were all male Massachusetts Institute of Technology undergraduate and graduate students. Before the experiments, the drivers were first given oral and written instructions describing the brake system and the task of the experiments. They were then given unlimited practice sessions until they felt confident to manipulate the brake pedal in a variety of situations that would appear in actual experiments. The practice sessions were followed by the three different experimental runs described above. Each experimental run was conducted for about 10 min with 5-min breaks between them.

E. Results of Simulation Experiments

The performance of the five driver–vehicle systems were compared in terms of the performance indexes such as road condition awareness and situation adaptability.

Fig. 15 illustrates typical phase-plane plots, where pedal-depression speed is plotted against pedal travel. These phase-plane plots compare the driver's pedal maneuver on dry and wet/icy roads. Plots are presented only for Models 2–4 since Model 1 and 5 have the same pedal stiffness on either dry or wet/icy road. Among these three models, Model 4 indicates the largest phase-plane difference for the two different road conditions; the area of the plot for the wet/icy road is much larger than that for the dry road. Model 3 shows a sudden change of pedal-depression speed, which appears as a spike just before full braking in Fig. 15(b). This indicates a sudden yielding of the pedal upon ABS activation as described in Section III-D. Model 2 indicates no substantial change in pedal depression on different road conditions. This phase-plane plot provides a good format for comparing the driver's kinesthetic perception. Since neuromuscular systems provide sensing of muscle stretch and stretch rate (spindle afferent) as well as force sensing (Golgi tendon afferent), the brake pedals in Models 3 and 4 provided the driver with a kinesthetic display of braking or road condition.

The drivers were questioned on road-surface conditions perceived and reported immediately after each braking situation. The ratings of the road condition estimates from nine drivers are listed in Fig. 16. Each point represents the sum across all situations in the specified experiments. It is evident from the ratings that the drivers perceived road conditions easily in Models 3 and 4. While there were variations in baselines among the drivers, for each driver, the ratings were considerably higher for Models 3 and 4. Especially in Model 4, the drivers recognized the road conditions correctly in most situations. This result can be explained by the discussion in Section III-D about the driver's kinesthetic perception. Clearly, change in the phase-plane portrait of pedal depression appears to help the drivers perceive the road-surface conditions.

From the *situation-adaptation experiment*, the drivers' situation adaptation for each model was evaluated. The ratings of the situation adaptation from eight drivers are given in Fig. 17. Each point represents the sum across all situations for each driver and model. Models 3 and 4 had high ratings with small variations among the drivers. Model 1 showed the largest variation among drivers.

The drivers appeared to perceive the road conditions more accurately under the proposed designs (Models 3 and 4). Also, the proposed designs appeared to help the driver's situation adaptability in various braking situations. Some of the drivers (Drivers B and H in Fig. 17), however, were able to acclimatize themselves to all the different brake systems so well that the system performance on the various systems could not be distinguished from one another.

Authorized licensed use limited to: MIT Libraries. Downloaded on August 12,2010 at 14:54:01 UTC from IEEE Xplore. Restrictions apply.

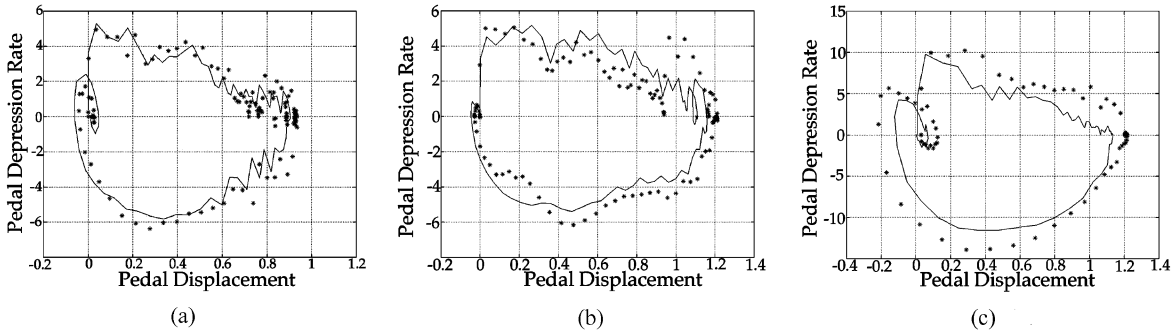

Fig. 15. Normalized phase-plane plots of brake-pedal depression on dry and wet/icy roads. (a) Model 2. (b) Model 3. (c) Model 4. (solid line: dry road; dotted line: wet/icy road).

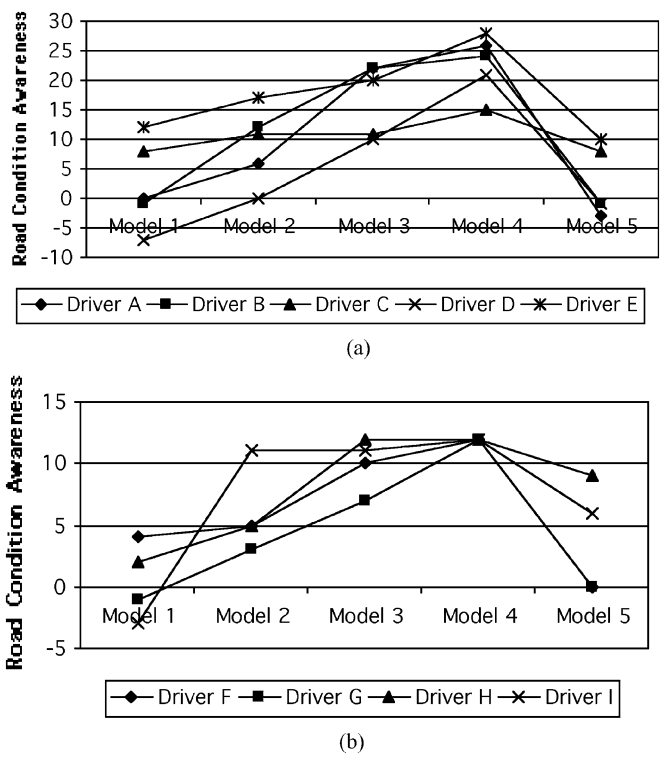

Fig. 16. Road-condition awareness results. (a) Ratings from all three experiments. (14 situations) (b) Ratings from *situation-adaptation experiment* only. (six situations).

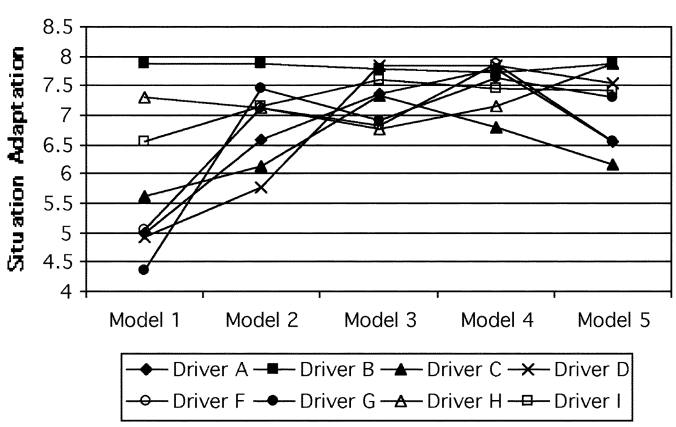

Fig. 17. Situation-adaptation results.

IV. Discussion

As a solution to the automobile collision avoidance problem, brake-assistance systems such as the ABS have become more and more popular on modern vehicles. ABS reduces the likelihood of the brake's locking the wheels and causing skidding and resulting in loss of steering ability in panic-stop situations. Thus, ABS provides the driver with an opportunity to steer out of emergencies. However, according to accident statistics, ABS-equipped cars might be worse than non-ABS-equipped cars in emergency braking situations. In their report to the National Highway Traffic Safety Administration [1], Hertz *et al.* reported that there has been no net crash reduction attributed to ABS. The Insurance Institute for Highway Safety [2] believed that cars with ABS are more likely than those without it to be involved in a fatal crash.

The poor performance of conventional brake systems with ABS seems to result from the open-loop nature of braking maneuvers. In braking, the driver depends on his senses (visual, vestibular, auditory, etc.) to receive information about ongoing traffic, and his task is to manipulate the brake pedal in order to stop his vehicle according to ongoing traffic. To produce a desired pedal displacement, the driver must produce a force determined by the mechanical stiffness or impedance of the brake pedal; to produce a desired force requires a particular displacement, also determined by the impedance. The impedance characteristic of the brake pedal has a strong effect on the driver's braking performance. In *manual* control studies, it is recommended that the control handle be designed so that the dynamics between force on the handle and handle displacement are similar to the dynamics between force on the handle and system output [30]. This makes the handle a *tactile-kinesthetic display* of output as well as an *input device* and provides better dynamic compatibility between system output and the operator's response. However, currently, the brake pedal is not designed to display the braking performance, but rather is only a simple input device. Even with ABS, pulsing at the brake pedal only indicates ABS activation; this signal does not serve as an intuitive cue of braking performance since vibration is commonly used as a warning or an indicator of malfunction of a system.

As a precursor study in brake-system design, this paper has examined the general features of human leg motion through experiments and numerical simulation. Analyzing a simple

Authorized licensed use limited to: MIT Libraries. Downloaded on August 12,2010 at 14:54:01 UTC from IEEE Xplore. Restrictions apply.

reaching motion of the leg helped illuminate the mechanisms underlying the driver's maneuver of the brake pedal. Findings from leg motion analysis have provided some new insight on brake-system design, which takes advantage of the open-loop nature of human motor control. It should be noted that the purpose of this leg-motion study was not to validate any particular motor control theory, but rather to explore and understand the representative properties of the driver's braking motion as it relates to the characteristics of human leg movement.

While there have been significant advances in automotive engineering thanks to recent development of electronics, the automobile has not yet evolved nearly as far as the aircraft in terms of automation and human supervisory control. In modern aircraft, the pilot controls the aircraft through computers, while the driver controls the vehicle rather directly. Aviation studies may provide us with ideas on how we could improve the ease and safety of the driving through automation and computerization. Automotive engineers are hoping for this improvement in the so-called "steer-by-wire" and "brake-by-wire" controls of the automobile. Since the concept of BBW allows us to tailor the characteristics of brake pedal arbitrarily, we can consider the possibility of modeling the brake system as a teleoperator.

In teleoperation studies, adaptive impedance at a master port and at a slave port is known to improve the performance of a contact task with an operator-telemanipulator system [3]. In this paper, an automotive brake system is considered to be a type of teleoperator performing a contact task. Based on teleoperation principles, this paper proposed two brake systems. The proposed designs account for the characteristics of human leg motion and kinesthetic feedback to the driver. The potential effectiveness of the proposed designs has been confirmed through the driving simulation. In driving simulation, the proposed designs appeared to help the driver perceive the road conditions more accurately. Also, the drivers could adapt to various braking situations more easily under the proposed designs.

V. Conclusion and Future Works

While ABS takes full advantage of the brake-control capabilities available with modern electronics, the human–machine interface for the ABS has not been designed to fully utilize the advanced features of the brake system. The goal of this study was to design brake systems that provide the driver with intuitive brake control and proper performance information. This paper proposes brake systems based on two new aspects. First, the braking motion of the driver is modeled and taken into consideration in designing the brake systems. Second, the brake system is considered as a teleoperator, providing proper feedback to the driver. The performance of the driver and vehicle as a combined system was examined using a driving simulator. It showed that the new brake systems helped the drivers perceive the road-surface conditions through the kinesthetic cue from the brake pedal.

As recommended future research, the authors propose improvements to the experimental procedure in leg-motion analysis and further studies on the impedance tuning of the brake pedal.

- Precise measurement of the interaction force between the foot and pedal will provide data for an accurate analysis of human motion under external perturbation. A computer-controlled robotic manipulator with force transducer can be used to apply external perturbations in leg motion and measure the interaction force [20]. The 2-D motion measurement employed in this study may be replaced by three-dimensional multijoint motion capture techniques.
- This study has shown that brake-pedal feel has great effects on perception of braking situation and, in turn, on braking performance of a combined system of driver–vehicle. Using BBW systems, the pedal feel can be arbitrarily tailored by decoupling the energetic interaction between actuator and control unit of brake-system. Further detailed studies should analyze how the impedance parameter of the brake-pedal should be tuned in BBW systems.

Acknowledgment

The authors would like to thank all the experimental subjects for their participation in our study. The first year of this work was supported by R. Bosch, GmbH. This support is gratefully acknowledged.

References

[1] E. Hertz, J. Hilton, and D. Johnson, "An analysis of the crash experience of passenger cars equipped with antilock braking systems," US Dept. Trans., NHTSA, DOT HS 808279, 1995.

[2] (1996) Antilock brakes don't reduce fatal crashes: People in cars with antilocks are at greater risk. *Insurance Inst. Highway Safety, News Release* [Online]. Available: http://www.hwysafety.org/news_releases/1996/pr121096.htm

[3] G. Raju, "Operator adjustable impedance in bilateral remote manipulation," Ph.D. dissertation, Dept. Mech. Eng., Mass. Inst. Technol., Cambridge, 1988.

[4] A. Bejczy and J. Salisbury, "Kinesthetic coupling between operator and remote manipulator," in *Proc. Int. Comput. Technol. Conf.* , vol. 1, 1980, ASME Century 2, pp. 197–211.

[5] N. Bernstein, *The Coordination and Regulation of Movements*. New York: Pergamon Press, 1967.

[6] M. Arbib, *The Metaphorical Brain: An Introduction to Artificial Intelligence and Brain Theory*. New York: Wiley Interscience, 1972.

[7] E. Saltzman, "Levels of sensorimotor representation," *J. Math. Psych.*, vol. 20, pp. 91–163, 1979.

[8] P. Morasso, "Spatial control of arm movements," *Exp. Brain Res.*, vol. 42, pp. 223–227, 1981.

[9] J. Hollerbach and C. Atkeson, "Deducing planning variables from experimental arm trajectories: Pitfalls and possibilities," *Biol. Cybern.*, vol. 56, pp. 279–292, 1987.

[10] J. Albus, "A new approach to manipulator control: The cerebellar model articulation controller (CMAC)," *J. Dynamics. Sys., Meas. Contr.*, vol. 97, pp. 220–227, 1975.

[11] M. Raibert, "A State Space Model for Sensorimotor Control and Learning,", MIT Artif. Intel. Memo, No. 351, 1976.

[12] E. Bizzi, N. Hogan, F. Mussa-Ivaldi, and S. Giszter, "Does the nervous system use equilibrium-point control to guide single and multiple joint movements," *Behav. Brain Sci.*, vol. 15, pp. 603–613, 1992.

[13] T. Flash, "The control of hand equilibrium trajectories in multi-joint arm movements," *Biol. Cybern.*, vol. 57, pp. 257–274, 1987.

[14] E. Pennisi, "Tilting against a major theory of movement control," *Science*, vol. 272, pp. 32–33, 1996.

[15] H. Gomi and M. Kawato, "Equilibrium-point control hypothesis examined by measured arm stiffness during multijoint movement," *Science*, vol. 272, pp. 117–120, 1996.

Authorized licensed use limited to: MIT Libraries. Downloaded on August 12,2010 at 14:54:01 UTC from IEEE Xplore. Restrictions apply.

[16] R. Shadmehr and F. Mussa-Ivaldi, "Adaptive representation of dynamics during learning of a motor task," *J. Biomech.*, vol. 29, pp. 1137–1146, 1994.

[17] F. Mussa-Ivaldi, "Motor primitives, force-fields and the equilibrium point theory," in *From Basic Motor Control to Functional Recovery*, N. Gantchev and G. N. Gantchev, Eds. Sofia, Bulgaria: Academic, 1999, pp. 392–398.

[18] W. Woodson and D. Conover, *Human Engineering Guide for Equipment Designers*. Berkeley: Univ. California Press, 1964.

[19] W. Abend, E. Bizzi, and P. Morasso, "Human arm trajectory formation," *Brain*, vol. 105, pp. 331–348, 1982.

[20] J. Won and N. Hogan, "Stability properties of human reaching movements," *Exper. Brain Res.*, vol. 107, pp. 125–36, 1995.

[21] J. Paines, "Optimization of manual control dynamics for space telemanipulation: impedance control of a force reflection hand controller," S.M. Thesis, Dept. Aeronaut. Astronaut., Mass. Inst. Technol., Cambridge, 1987.

[22] F. Mussa-Ivaldi, N. Hogan, and E. Bizzi, "Neural, mechanical, and geometric factors subserving arm posture in humans," *J. Neurosci.*, vol. 5, no. 10, pp. 2732–2743, 1985.

[23] A. Feldman, "Functional tuning of the nervous system with control of movement or maintenance of a steady posture, II: Controllable parameters of the muscle," *Biophysics*, vol. 11, pp. 565–578, 1966.

[24] E. Bizzi, N. Accomero, W. Chapple, and N. Hogan, "Posture control and trajectory formation during arm movement," *J. Neurosci.*, vol. 4, pp. 2738–2744, 1984.

[25] J. McConville, T. Churchill, I. Kaleps, C. Clauser, and J. Cuzzi, "Anthropometric relationships of body and body segment moments of inertia," Anthropol. Res. Project, Inc; Aerospace Med. Div., AFSC, Tech. Rep. No. AFAMRL-TR-80-119, 1980.

[26] T. Sheridan, *Telerobotics, Automation, and Human Supervisory Control*. Cambridge, MA: MIT Press, 1992.

[27] W. Barfield and T. Furness, *Virtual Environments and Advanced Interface Design*. London, U.K.: Oxford Univ. Press, 1995.

[28] C. Ciamberlini, G. Innocenti, and G. Longobardi, *Rev. Scientif. Instr.*, vol. 66, pp. 2684–2689, 1995.

[29] T. Tabe, N. Ohka, H. Kuraoka, and M. Ohba, "Automotive antiskid system using modern control theory," in *Proc. IEEE IECON*, 1985, pp. 390–395.

[30] J. Herzog, "Manual control using the matched manipulator control technique," *IEEE Trans. Man–Machine Syst.*, vol. 9, no. 3, pp. 56–60, 1968.

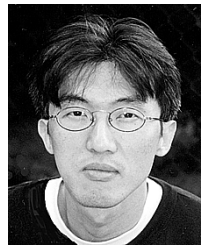

Shinsuk Park received the B.S. and M.S. degrees in mechanical design and production engineering from Seoul National University, Seoul, Korea, in 1989 and 1991, respectively, and the Ph.D. degree in mechanical engineering from Massachusetts Institute of Technology (M.I.T.), Cambridge, in 1999.

He served as a Post-Doctoral Research Fellow at Biorobotics Laboratory, Harvard University, Cambridge, MA, from 2000 to 2002. He was a Visiting Assistant Professor in the Department of Mechanical Engineering, Keio University, Japan, from 2002 to 2004. Currently, he is an Assistant Professor in the Department of Mechanical Engineering, Korea University, Seoul. His research interests include dynamics systems and control and their applications to human–machine interface design and biomedical engineering problems.

Thomas B. Sheridan (M'60–SM'82–F'83–LF'96) received the B.S.M.E. degree from Purdue University, West Lafayette, IN, in 1951, the M.S.Eng. degree from the University of California, Los Angeles, in 1954, the Sc.D. degree from the Massachusetts Institute of Technology (MIT), Cambridge, in 1959, and the Dr. (honorary) from Delft University of Technology, Delft, Netherlands.

He is a Ford Professor of Engineering and Applied Psychology Emeritus, Department of Mechanical Engineering and the Department of Aeronautics and Astronautics, MIT. He is coauthor of *Man-Machine Systems* (USSR: MIT Press, 1974, 1981), coeditor of *Monitoring Behavior and Supervisory Control* (New York: Plenum, 1976), author of *Telerobotics, Automation, and Human Supervisory Control* (Cambridge, MA: MIT Press, 1992), coeditor of *Perspectives on the Human Controller* (Mahwah, NJ: Erlbaum, 1997) and author of *Humans and Automation* (New York: Wiley, 2002).

Dr. Sheridan is a Fellow of the Human Factors and Ergonomics Society (HFES) and a Member of the National Academy of Engineering. He was President of the IEEE Systems, Man and Cybernetics Society and the HFES. He received the Norbert Wiener and Joseph Wohl Awards, the IEEE Centennial and Millennium Medals, the National Engineering Award of the American Association of Engineering Societies, and the Oldenburger Medal of ASME. He was the Editor of the IEEE TRANSACTIONS ON MAN–MACHINE SYSTEMS.

Authorized licensed use limited to: MIT Libraries. Downloaded on August 12,2010 at 14:54:01 UTC from IEEE Xplore. Restrictions apply.